INL/CON-23-74922-Revision-0

Integration of Condition-Based, Diagnostic, Prognostic, And Anomaly Detection Data into Reliability Models to Support a Predictive Maintenance Context

Changing the World's Energy Future

Diego Mandelli, Vivek Agarwal, Congjian Wang, Linyu Lin

INL/CON-23-74922-Revision-0

Integration of Condition-Based, Diagnostic, Prognostic, And Anomaly Detection Data into Reliability Models to Support a Predictive Maintenance Context

Diego Mandelli, Vivek Agarwal, Congjian Wang, Linyu Lin

October 2024

Idaho National Laboratory
Idaho Falls, Idaho 83415

http://www.inl.gov

Prepared for the
U.S. Department of Energy
Under DOE Idaho Operations Office
Contract DE-AC07-05ID14517

Integration of Condition-based, Diagnostic, Prognostic, and Anomaly Detection Data into Reliability Models to Support a Predictive Maintenance Context

D. Mandelli*, C. Wang, V. Agarwal, L. Lin
Idaho National Laboratory, Idaho Falls, Idaho, U.S.A.
*Corresponding Author: Diego.Mandelli@inl.gov

Abstract

Reliability data employed in plant reliability models neglect the present status of asset health (available, for example, from online monitoring data and diagnostic assessments) as well as any forecasted health projections (when available from prognostic models). Ideally, in a predictive maintenance context, system reliability models should support decision making by propagating actual health information from the asset to the system level in order to provide a quantitative snapshot of system health and to identify the most critical assets. Asset health should be informed solely by that specific asset's current and historical performance data and should not be an approximated integral representation of past industry-wide operational experience (as currently performed by system reliability models through Bayesian updating processes). This paper proposes a reliability modeling approach that relies on asset diagnostic and prognostic assessments, along with monitoring data to measure asset health. We show how state-of-the-art condition-based, diagnostic, prognostic, and anomaly detection models can be linked to system reliability models—not in probability terms, but in terms of margin (with margin being defined as the "distance" between the present status and an undesired event [e.g., failure or unacceptable performance]). We then show how margin data are propagated from the asset to the system level via classical reliability models such as fault trees (FTs) or reliability block diagrams. The described method can in fact propagate heterogenous health data from the asset to the system level in order to analytically assess system health.

Keywords: reliability, diagnostic, prognostic, condition-based, predictive maintenance

1. Introduction

Health management of complex systems such as nuclear power plants is essential for guaranteeing system reliability. This task can be greatly enhanced by constantly monitoring asset status/performance, then processing the resulting data (via anomaly detection and diagnostic/prognostic computational algorithms) to identify asset degradation trends and faulty states. While such data are typically available for many assets, they are not effectively propagated from the asset to the system level in order to identify the most critical assets and prioritize maintenance and surveillance activities. This is primarily because current reliability modeling techniques are inadequate for processing such information/data, as these techniques are based on the concept of failure probability and do not align with an operational context in which quantitative asset health information is available. Simply stated, current reliability techniques [Lee, 2011] serve a run-to-failure operational setting, not a predictive maintenance one in which the goal is to perform maintenance and surveillance activities only when deemed necessary due to asset health. Our work focuses on developing a different type of reliability modeling technique—one designed to support a predictive operational setting. This technique entails moving away from a failure probability mindset and toward a margin-based one [Mandelli, 2023]. In this context, "margin" is an analytical metric for quantifying asset health based solely on current and past operational experience pertaining to the asset being considered. Margin-based reliability techniques can propagate asset health information to the system level, as well as apply analytical importance measures to each asset. This paper presents several approaches usable to assess asset margin when provided condition-based, diagnostic, prognostic, or anomaly detection data.

2. Margin-based Reliability Modeling

[Mandelli 2023] expanded the meaning of the word "reliability" to better reflect the needs of system health and asset management decision-making processes. Rather than focusing on the likelihood of a given event (in probabilistic terms), we think in terms of how far off the event is from occurring. This new interpretation of reliability shifts the focus away from probability of occurrence and toward assessments of how near assets are to failure or at least reaching an unacceptable level of performance (see Figure 1). Note that two data elements are required for this assessment: the estimated actual health condition of the asset, which can be acquired by the asset-monitoring system or through diagnostic methods, and the limiting conditions that must be avoided, which can be acquired from past operational experience (e.g., monitoring data generated by similar assets under failure conditions).

An asset's margin value M (see Figure 1) is defined over the $[0,1]$ interval, where $M = 1$ corresponds to a perfectly healthy asset (requiring minimal to no maintenance attention) and $M = 0$ corresponds to a faulty asset (requiring maintenance attention). Note that margin quantification is impacted by the availability of monitoring data and can be defined over heterogenous variables such as pressure, vibration spectra, and time. For example, when dealing with condition-based monitoring data (both current and archived), margin M is here defined as the distance between actual and past conditions (e.g., oil temperature and vibration spectrum) that lead to failure (see Figure 1). Hence, margin-based reliability modeling provides a unified approach to dealing with heterogeneous monitoring data elements.

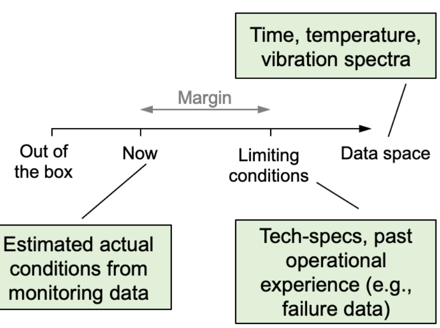

Figure 1. Graphical representation of margin, based on actual asset-monitoring data.

An asset's margin value is not static, but changes with time—depending on asset conditions. For example, if degradation due to usage is observed from the monitoring data, the corresponding asset margin value decreases. Conversely, if a maintenance operation is performed on that same asset (e.g., restoration of centrifugal pump bearings), the asset margin value increases. This mindset shift regarding the concept of reliability (i.e., margin based instead of probability based) offers the advantage of directly linking the asset health evaluation process to standard plant processes for managing plant performance (e.g., plant maintenance operations and budgeting processes). The transformation also supports decision making in a form that is more familiar and readily understandable to plant system engineers and decision makers.

Thus far, margin has been defined for one single asset. The next step is to quantify the system's margin value after obtaining the margin values of its assets. Margin values are not propagated from the asset level to the system level via set theory-based operations, but by employing classical reliability models such as fault trees (FTs) or reliability block diagrams [Lee, 2011], which are solved using different rule sets [Mandelli, 2023].

In this respect, margin-based operators for assets in both series (OR operator) and parallel (AND operator) configurations must be defined. As an example, consider two assets (A and B). The margin M of both assets can be visualized in a 2D space, as shown in Figure 2. Starting with brand-new assets (i.e., $M_A, M_B = 1$), the aging and degradation that affects both is represented by the blue line in the figure, which parametrically signifies the combination of both margins $M_A(t)$ and $M_B(t)$ at a specific point in time *t*. Note that if no maintenance (preventive or corrective) was ever performed on either asset, this path would move from coordinates $(1,1)$ to coordinates $(0,0)$, at which point both assets would be considered failed. Hence, the coordinates $(0,0)$ in Figure 2 represent the event $A\ AND\ B$. Similarly, when the blue line reaches the *x*- or *y*-axis of Figure 2 (characterized by $M_B = 0$ and $M_A = 0$, respectively), either asset A or B has failed. Hence, the points in Figure 2 characterized by either $M_B = 0$ or $M_A = 0$ represent the event $A\ OR\ B$.

We can now calculate the margin M for the AND and OR events described above. This is accomplished by following the definition of margin: by measuring the distance between the actual condition of assets A and B and the conditions identified by the event under consideration (i.e., the occurrence of both or either event[s]). The margin for $A\ AND\ B$ can be calculated as the distance between the current point (M_A, M_B) and point $(0,0)$, whereas the margin for $A\ OR\ B$ is the minimum distance from the current point (M_A, M_B) to the *x*- or *y*-axis of Figure 2 (where $M_B = 0$ and $M_A = 0$, respectively):

$$M(A\ AND\ B) = dist[(M_A, M_B), (0,0)] \tag{1}$$

$$M(A\ OR\ B) = min(M_A, M_B) \tag{2}$$

where the function $dist[.,.]$ indicates the metric designed for calculating the distance between two points in a Euclidean space (e.g., if Euclidean distance is employed, $M(A\ AND\ B) = \sqrt{M_A^2 + M_B^2}$). Mandelli (2022) provided a set of considerations regarding the appropriate distance metric $dist[.,.]$ to be employed. In summary, Euclidean and Manhattan distance metrics represent the lower and upper bounds for $M(A\ AND\ B)$ (i.e., $\sqrt{M_A^2 + M_B^2} \leq M(A\ AND\ B) \leq M_A + M_B$). If the temporal evolution of M_A and M_B is available, a more precise estimate of $M(A\ AND\ B)$ can be obtained. Equations (1) and (2) allow us to propagate margin values via classical reliability models (e.g., FTs or reliability block diagrams) in order to quantify the system margin M_{sys}.

The definition of margin given thus far is abstract; application within a more practical setting depends on the phenomena of interest—and especially the monitoring data available. The following sections provide more quantitative details on how margin can be quantified based on the available equipment reliability (ER) data.

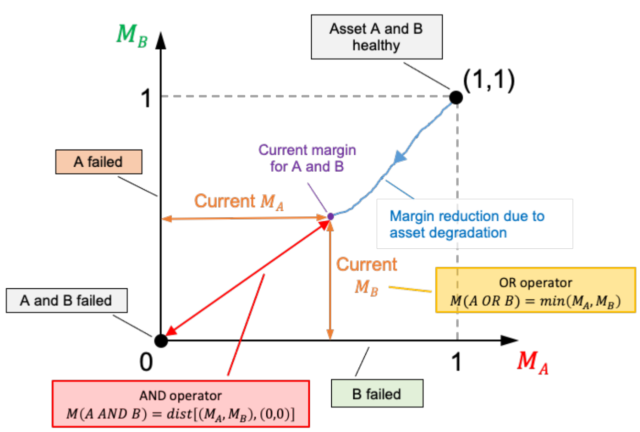

Figure 2: Graphical representation of event occurrences, based on a margin framework.

Reliability models (e.g., FTs and reliability block diagrams [Lee, 2011]) can be solved symbolically by generating the minimal cut sets (MCSs) of the considered system and then applying Equations (1) and (2) to numerically determine the margin of each MCS, as well as that of the union of all the MCSs. In the context of margin-based reliability modeling, rather than considering the system MCSs, it is more suitable to rely on the concept of minimal path sets (MPSs) [Youngblood, 2001]. From a reliability standpoint, these two concepts are strongly related: MCSs represent conditions under which the system can fail (failure paths), while MPSs represent conditions under which the system can effectively operate (i.e., success paths). More precisely, a MCS represents a subset of assets that, once all failed, cause the system to fail. Conversely, a MPS represents a subset of assets that, when all functioning, guarantee the system to be functional. As the concept of margin is intended for measuring asset health, it focuses on asset operability. When focusing on continuously operating systems (e.g., the secondary side of nuclear power plants), it is relevant—from a decision-making point of view—to identify ways of guaranteeing successful system operation. Hence, MPSs coupled with margin-based calculations are more suitable in a predictive maintenance context.

3. Technical Specifications Data

In many practical settings, the limiting conditions shown in Figure 1 can be represented by the technical specifications of the considered asset, which are normally provided by the manufacturer. For example, to ensure proper function of the induction motors, the oil viscosity, which can significantly change as a function of motor rotation speed, must be below the specified limiting condition.

As indicated in Section 2, margin can be calculated as the distance between the actual and the limiting conditions. In this context, the asset margin can be calculated as the difference between the currently measured oil viscosity and the limiting condition listed in the technical specifications. Given an upper limiting condition x_{LC} for a monitored variable x_{obs}, a margin M can be defined as:

$$M(x_{obs}) = \frac{x_{LC} - x_{obs}}{x_{LC} - \min(x_{obs})} \tag{3}$$

where $\min(x_{obs})$ indicates the minimum allowable value for x_{obs}.

For example, induction motors are designed to operate within specified differential temperature limits. These limits indicate the maximum permissible difference between the motor temperature and the environmental temperatures that various classes of insulation materials are able to withstand (this temperature limit can range from 80°C to 120°C, depending on the insulation material). In this scenario, x_{LC} is represented by the specified temperature limit and x_{obs} is the difference between the actual motor temperature and the environmental temperature.

4. Anomaly Detection Data

Here, we consider a case in which the available monitoring data for the asset being considered were collected exclusively when the asset was healthy $\Xi^{obs-healthy}$, meaning that data pertaining to asset degradation or failure are unavailable. $\Xi^{obs-healthy}$ represents a collection of past observation data elements ξ^{obs}. The following notation is used throughout this paper: a single observation data element ξ^{obs} can be composed of L observed variables, $\xi^{obs} = [x_1, .., x_L]$, and the observed variables x_l $(l = 1, ..., L)$ can be heterogenous in nature (e.g., temperature, pressure).

In this kind of situation, an asset's health status can be established by measuring how actual monitoring data differ (distance-wise) from healthy data. In this respect, anomaly detection tools [Nassif, 2021] can be used to quantify the residual between the actual observed data ξ^{obs} and the predicted data ξ^{rec} (as computed from ξ^{obs} and $\Xi^{obs-healthy}$). Such tools can be based on a kernel density estimation (e.g., the auto-associative kernel regression method [Baraldi, 2015]) or on deep-learning-based methods (see [Zhang, 2019], among others). Under normal conditions, ξ^{rec} is very similar to ξ^{obs} (i.e., $\xi^{obs} \cong \xi^{rec}$), meaning that $\xi^{obs} \neq \xi^{rec}$ indicates anomalous behavior (e.g., asset degradation).

In this context, a margin value can then be defined as the distance between ξ^{rec} and ξ^{obs}:

$$M(\xi^{obs}) = e^{-\left(\frac{\left\|\xi^{obs}-\xi^{rec}\right\|}{h}\right)^2} \tag{4}$$

where $\left\|\xi^{obs} - \xi^{rec}\right\|$ indicates the residual between the observed and the predicted data, and h represents the comparison parameter between ξ^{rec} and ξ^{obs} (expressed in terms of standard deviation). When the asset is experiencing normal conditions (i.e., $\xi^{obs} \cong \xi^{rec}$), $M = 1$. If the asset is experiencing abnormal conditions, the norm of the difference between ξ^{obs} and ξ^{rec} increases, causing M to drop to 0.

Note that $\Xi^{obs-healthy}$ is here assumed to cover all possible healthy asset conditions. If this is not actually the case, when ξ^{obs} enters an unforeseen healthy condition, the obtained margin value will show the asset to be unhealthy. However, once the newly observed healthy conditions are recorded, they can be added to the original dataset $\Xi^{obs-healthy}$.

Figure 3 reflects a set $\Xi^{obs-healthy}$ of observed data elements $\xi^{obs} = [x_1, x_2]$ being collected (the green dots in the left-hand image). Actual observed data ξ^{obs} are constantly recorded, while ξ^{rec} are determined based on ξ^{obs} and $\Xi^{obs-healthy}$ (see the black and red lines in the left-hand image), using the auto-associative kernel regression method [Baraldi, 2015]. Applying Equation (6) to this test case enables a temporal profile to be generated for the corresponding margin (see the right-hand image).

Note that the definition of margin presented in Equation (6) can be adapted and/or redefined depending on the machine learning (ML) model [Mohri, 2012] (e.g., KNN, SVM, ANN, CNN) employed by the anomaly detection method (either supervised or unsupervised). In most situations, the output of a generic anomaly detection method can be written in the form of the Boolean variable out (indicating whether ξ^{obs} was observed under normal or abnormal conditions), and a variable C^{obs} (indicating the degree of confidence in the prediction). In such cases, given an anomaly detection method, a generic formulation of the margin associated with an observation ξ^{obs} can be expressed as follows:

$$M\left(\xi^{obs}\right) = \begin{cases} 0.5 - \frac{C^{obs}}{2} & if\ out = abnormal \\ 0.5 + \frac{C^{obs}}{2} & if\ out = normal \end{cases} \tag{5}$$

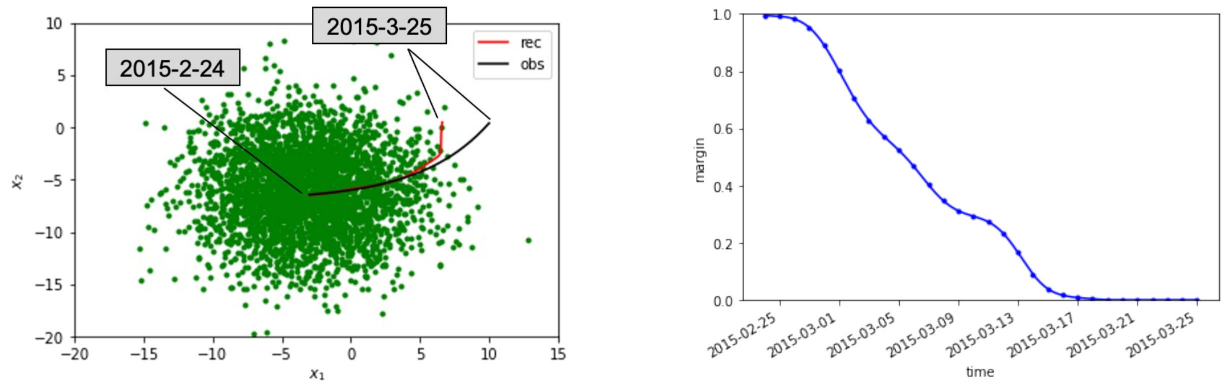

Figure 3. (Left) Representation of $\Xi^{obs-healthy}$ (green population), ξ^{obs} (black line), and ξ^{rec} (red line) in the x_1, x_2 space. (Right) Temporal profile of the corresponding margin.

5. Condition-based Data

In this scenario, by following the definition of margin given in Section 2—and by being provided actual observed data (containing both historic healthy $\Xi^{obs-healthy}$ data and faulty data $\Xi^{obs-faulty}$)—a margin value can be determined by comparing the mutual distance of ξ^{obs} from the two populations: $\Xi^{obs-healthy}$ and $\Xi^{obs-faulty}$ (see Figure 4). Note that this case extends the one described in Section 4 (in which only data generated under healthy conditions $\Xi^{obs-healthy}$ were available) by incorporating data generated under faulty conditions, indicated here as $\Xi^{obs-faulty}$. It is assumed that, in the presence of an asset fault, the actual observed data ξ^{obs} can be seen transitioning from $\Xi^{obs-healthy}$ to $\Xi^{obs-faulty}$.

Without loss of generality and assuming both $\Xi^{obs-healthy}$ and $\Xi^{obs-faulty}$ to be well-structured datasets, a margin can be written as:

$$M(\xi^{obs}) = \frac{D(\xi^{obs};\Xi^{obs-faulty})}{D(\xi^{obs};\Xi^{obs-faulty}) + D(\xi^{obs};\Xi^{obs-healthy})} \quad (6)$$

where the operator $D(.;.)$ represents the distance between one single data element (i.e., ξ^{obs}) and a population of data elements (either $\Xi^{obs-healthy}$ or $\Xi^{obs-faulty}$). The choice of operator $D(.;.)$ may depend on several factors, as dictated by the distribution of the $\Xi^{obs-healthy}$ and $\Xi^{obs-faulty}$ populations in the data space. Note that the model presented in Equation (6) is basically distance based, and does not directly employ any type of ML model. Note also that a distance-based approach for $D(\xi^{obs};\Xi)$ is only effective when the healthy and faulty data are well separated from each other in the $[x_1, .., x_L]$ space.

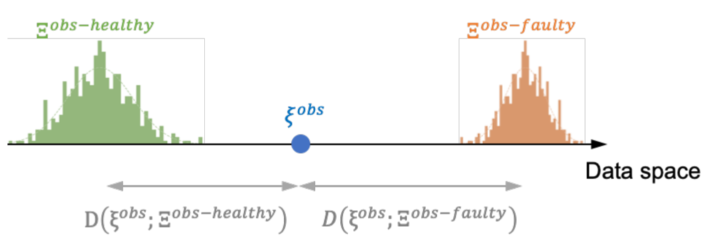

Figure 4. Margin calculation, given the current status of the monitored asset ξ^{obs} when both healthy $\Xi^{obs-healthy}$ and faulty $\Xi^{obs-faulty}$ data are available in the $[x_1, .., x_L]$ data space.

In practical scenarios, however, these two populations of data elements may overlap. In such cases, margin can be quantified using density-based methods [Hastie, Tibshirani, and Friedman, 2001], which are designed to translate (e.g., via kernel density estimation methods) the $\Xi^{obs-healthy}$ and $\Xi^{obs-faulty}$ datasets into probability distribution functions (PDFs) $pdf^{healthy}$ and pdf^{faulty}. Then, given a current observed measurement ξ^{obs}, margin can be quantified by evaluating these two PDFs at the coordinate ξ^{obs}:

$$M(\xi^{obs}) = \frac{pdf^{healthy}(\xi^{obs})}{pdf^{healthy}(\xi^{obs}) + pdf^{faulty}(\xi^{obs})} \quad (7)$$

This equation weighs the PDF values at coordinate ξ^{obs} under both healthy and faulty conditions. When ξ^{obs} is located in a region of the $[x_1, .., x_L]$ space dominated by healthy data, $pdf^{healthy}(\xi^{obs}) \gg pdf^{faulty}(\xi^{obs})$ and $M(\xi^{obs}) \cong 1.0$. Conversely, when ξ^{obs} is located in a region of the $[x_1, .., x_L]$ space dominated by faulty data, $pdf^{healthy}(\xi^{obs}) \ll pdf^{faulty}(\xi^{obs})$ and $M(\xi^{obs}) \cong 0.0$.

In the example given in Figure 5, $\Xi^{obs-healthy}$ and $\Xi^{obs-faulty}$ are shown in the left-hand plot, ξ^{obs} is represented as the black line moving from left to right, and the corresponding margin is shown in the right-hand plot. Here, $pdf^{healthy}(\xi^{obs})$ and $pdf^{faulty}(\xi^{obs})$ were generated using kernel density estimation methods (Hastie, Tibshirani, and Friedman, 2001).

An alternative formulation to Equation (7) can be derived when ML methods are employed. In this setting, a supervised ML model (i.e., a classifier) is trained using both the faulty and healthy datasets ($\Xi^{obs-faulty}$, $\Xi^{obs-healthy}$) and is then employed to predict, given ξ^{obs}, the class out (either faulty or healthy) to which ξ^{obs} belongs. Such a prediction can be augmented by also determining the probability estimate $Prob^{detec}$ associated with the predicted out. If the [0,1] margin interval is divided into two equally long segments, we can assign the "healthy" class to the [.5,1] interval and the "faulty" class to the $[0, .5]$ interval. Hence, the predicted class out generated by the ML model determines the margin variability interval (either $[0, .5]$ or [.5,1]). The variable $Prob^{detec}$ (see Figure 6) is essentially a measure of the prediction accuracy. More precisely, a high value of $Prob^{detec}$ implies a high degree of accuracy in the prediction; conversely, a very low value implies low accuracy. In this context, $Prob^{detec}$ is used to determine the precise margin location in the $[0, .5]$ or [.5,1] intervals. A high value of $Prob^{detec}$ would drive the margin toward the extremes of the intervals (either 0 or 1), whereas a low value would drive it toward the common point of the intervals (i.e., 0.5).

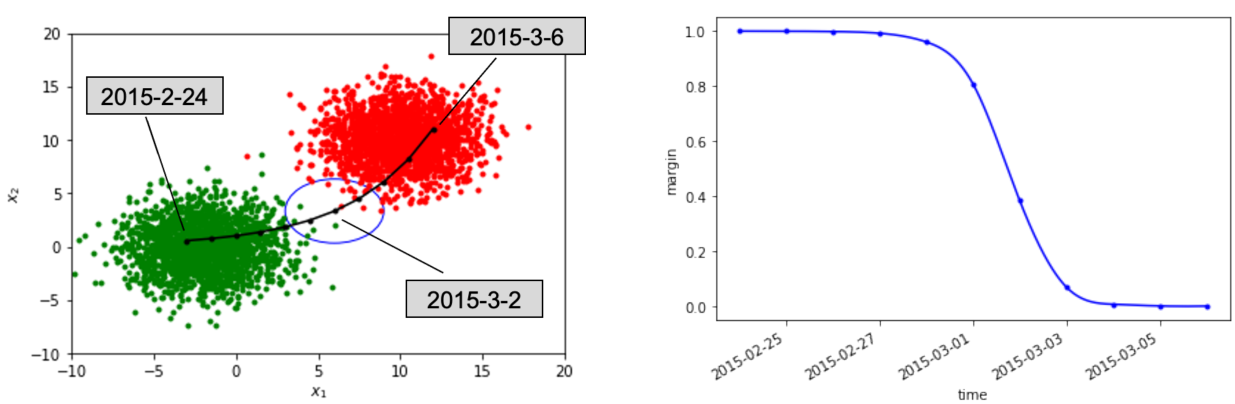

Figure 5. (Left) Representation of $\Xi^{obs-healthy}$ (green population), $\Xi^{obs-faulty}$ (red population), and ξ^{obs} (black line) in the x_1, x_2 space. (Right) Temporal profile of the corresponding margin.

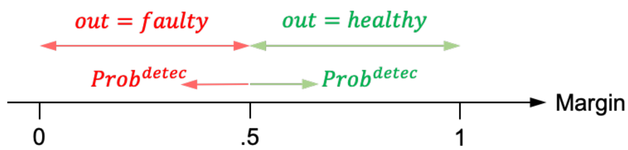

Figure 6. Graphical representation of margin, based on the out and $Prob^{detec}$ values predicted by a ML model.

Provided ξ^{obs} and a ML model that can generate both out and $Prob^{detec}$, a margin value can thus be defined as:

$$M(\xi^{obs}) = \begin{cases} 0.5 - \frac{Prob^{detec}}{2} & if\ out = faulty \\ 0.5 + \frac{Prob^{detec}}{2} & if\ out = healthy \end{cases} \tag{8}$$

Deep-neural-network-based models [Hastie, Tibshirani, and Friedman, 2001] are an ML model class widely employed for diagnostic applications. Given ξ^{obs}, this class of classifier models generates the class out (either faulty or healthy) to which ξ^{obs} belongs, along with a probability value associated with each class: $Prob^{healthy}$ and $Prob^{faulty}$ (rather than the single probability value $Prob^{detec}$). Note that, if two classes are considered (faulty and healthy), $Prob^{healthy} + Prob^{faulty} = 1$. The variable out is calculated per:

$$out = \begin{cases} healthy & if\ Prob^{healthy} > Prob^{faulty} \\ faulty & if\ Prob^{healthy} < Prob^{faulty} \end{cases} \tag{9}$$

In this context, margin quantification directly employs the two generated probability values (i.e., $Prob^{healthy}$ and $Prob^{faulty}$), per:

$$M(\xi^{obs}) = Prob^{healthy} = 1 - Prob^{faulty} \tag{10}$$

6. Prognostic Data

Estimating an asset's remaining useful life (RUL) provides valuable information on when exactly that asset can be expected to experience loss of function. Given the stochastic nature of the failure phenomena, RUL is typically expressed in terms of a probabilistic distribution along the temporal axis. Many methods have been developed in the literature to predict RUL for specific assets, and [Ferreira and Gonçalves 2022] summarize the most widely used methods. To integrate the RUL PDF (indicated here as PDF_{RUL}) into a margin-based reliability model, we apply reasoning similar to that presented in Section 2. Here, a margin is the distance between the actual time and the predicted RUL. The main differences are that the RUL is estimated once a degradation mechanism has been identified (e.g., using an anomaly detection method) and is an actual distribution function rather than a point value.

Once the RUL PDF is predicted, the corresponding margin value can be estimated via two approaches. The first defines the margin as:

$$M(t) = 1 - CDF_{RUL}(t) \tag{11}$$

where CDF_{RUL} indicates the cumulative distribution function corresponding to PDF_{RUL}. The second approach estimates margin as the distance between the actual asset life and a point estimate of the RUL distribution:

$$M(t) = \frac{p_{5\%}^{RUL} - t}{p_{5\%}^{RUL}} \quad (12)$$

where $p_{5\%}^{RUL}$ indicates the 5th percentile of the RUL distribution PDF_{RUL}.

Figure 7 shows a graphical representation of the margins for both approaches in regard to an estimated RUL (in red) that is normally distributed. Note that the proposed approach updates the margin value when the asset health is measured, and consequently a better RUL estimation (i.e., one featuring less uncertainty associated with the RUL) is calculated by the corresponding prognostic model.

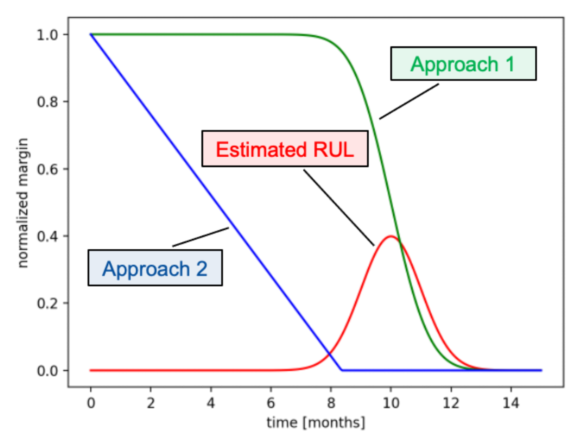

Figure 7. Margin values obtained via the two proposed approaches (green and blue lines), given an estimate of the asset's RUL (red line).

Before initial degradation is detected (meaning the RUL cannot yet be estimated), the asset margin is set to 1.0 (asset healthy). Once asset degradation is observed and RUL PDF estimation becomes available, the corresponding margin value is updated using the same estimators indicated in Equations (11) and (12).

7. Example of Margin-based Reliability Analysis

Here, we present an example of margin-based reliability calculation for the system shown in Figure 8 [Youngblood, 2001], which is comprised of seven assets, A–G. The top plot in Figure 9 shows an estimation of each asset's RUL. Here, RUL estimations are represented probabilistically, meaning that RUL is represented by a PDF designed to reflect the uncertainty associated with RUL estimates (in terms of RUL mean and variance). In this scenario, we represent system reliability in terms of MPSs rather than MCSs. The system margin is calculated considering the MPSs of the system shown in Figure 8, and by applying the margin rules indicated in Section 2 (i.e., the margin of each asset is calculated from its RUL by applying Equation (11).

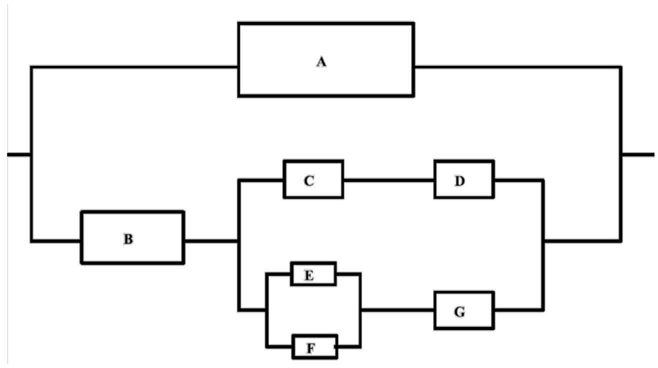

Figure 8. Example of the system architecture as represented in terms of block diagrams [Youngblood, 2001].

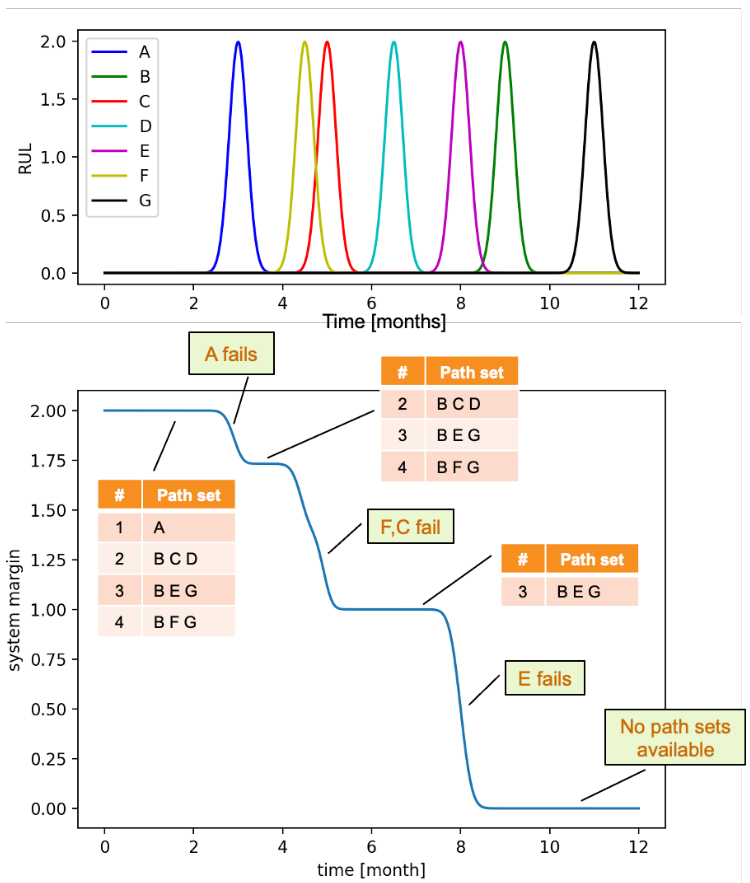

Figure 9. Example of margin-based calculations based on prognostic data for the system indicated in Figure 8, with the top plot showing the estimated RUL for each of the seven assets (A–G) and the bottom plot indicating the corresponding quantification of system margin.

The obtained temporal profile of system margin is shown in the bottom plot of Figure 9. Note that:

- Even though the asset margin is defined in the [0,1] interval, the system margin can exceed 1 (though it still cannot be negative). A system margin of greater than 1 indicates redundancies that compensate for asset failures. In other words, when there are multiple MPSs, the system margin will exceed 1. At time $t = 0$, there are four MPSs and the margin for each asset is set to 1. Hence the system margin can be calculated as $\sqrt{1 + 1 + 1 + 1} = 2.0$.

- When assets approach the end of their RUL, their margins decrease to 0, at which point they are considered failed. Hence, the number of available MPSs decreases, as do the system margins until reaching a value equal to square root of the number of available MPSs.

- At time $t = 8\,months$, asset E fails. And even though assets B and G are working properly, the fact there are no available MPSs causes the system margin value to drop to 0.

8. Conclusions

This paper briefly presented a margin-based reliability approach designed to integrate condition-based, diagnostic, prognostic, and anomaly detection models. We began by presenting a margin-based approach for assessing asset health, based solely on actual and historic monitoring data (e.g., condition-based, anomaly detection, diagnostic, and prognostic data). We explained how heterogenous equipment reliability data elements and ML models can be employed to assess asset status via a margin value that serves as an analytical measure of asset health. We then showed how, depending on the operational context of the asset (e.g., type of failure modes) and the available health data pertaining to it, a margin value can be quantified using well-known statistical and ML algorithms. System health assessments are performed by propagating, via classical reliability models (e.g., FTs or reliability block diagrams), the margin values of those assets that support the system function(s). Such propagation is not performed via set theory-based rules, but rather through distance-based operations. The resulting information can then be used to assess the reliability importance of each asset in order to identify which are the most critical. A margin-based approach directly addresses the limitations of classical reliability modeling approaches and provides a snapshot of system health (given the availability of monitoring data). A margin-based interpretation of reliability shifts the focus of the concept away from probability of occurrence and toward assessing how far away (or close) an asset is to reaching an unacceptable level of performance or undergoing failure. This shift in focus provides a direct link between the asset/system health evaluation process and standard plant processes for managing plant performance (e.g., plant maintenance and budgeting processes).

References

Baraldi, P., F. Di Maio, P. Turati, and E. Zio. (2015). “Robust Signal Reconstruction for Condition Monitoring of Industrial Components via a Modified Auto Associative Kernel Regression Method.” *Mechanical Systems and Signal Processing*, Elsevier, 60-61, pp. 29-44. https://doi.org/10.1016/j.ymssp.2014.09.013.

Ferreira, C. and G. Gonçalves. (2022). “Remaining Useful Life Prediction and Challenges: A Literature Review on the Use Of Machine Learning Methods.” *J. Manuf. Syst.*, 63, pp. 550-562. https://doi.org/10.1016/j.jmsy.2022.05.010.

Hastie, T., R. Tibshirani, and J. Friedman. (2001). *The Elements of Statistical Learning*. New York, NY: Springer, pp. 193-224. https://doi.org/10.1007/978-0-387-21606-5_7.

Lee, J. C. and N. J. McCormick. (2011). *Risk And Safety Analysis of Nuclear Systems*. ISBN: 978-0-470-90756-6, Wiley, pp. 504. https://www.wiley.com/en-us/Risk+and+Safety+Analysis+of+Nuclear+Systems-p-9780470907566.

Mandelli, D., C. Wang, and S. Hess. (2023). “On the Language of Reliability: A System Engineer Perspective.” *Nuclear Technology*. Taylor and Francis Group, LLC. https://doi.org/10.1080/00295450.2022.2143210.

Mohri, M., A. Rostamizadeh, A. Talwalkar. (2012). *Foundations of Machine Learning*. ISBN: 9780262018258, MIT Press, 2012. https://mitpress.mit.edu/9780262018258/foundations-of-machine-learning/.

Nassif, A. B., M. A. Talib, Q. Nasir, F. M. Dakalbab. (2021). "Machine Learning for Anomaly Detection: A Systematic Review." in *IEEE Access*, vol. 9, pp. 78658–78700. https://doi.org/10.1109/ACCESS.2021.3083060.

Rausand, M., A. Barros, and A. Hoyland. (2020). *System Reliability Theory: Models, Statistical Methods, and Applications*. Wiley. https://doi.org/10.1002/9781119373940.

Siu, N., and Kelly D. (1998). "Bayesian Parameter Estimation in Probabilistic Risk Assessment." *Reliability Engineering and System Safety*, 62(1–2), pp. 89-116. https://doi.org/10.1016/S0951-8320(97)00159-2.

Xingang, Z., J. Kim, K. Warns, X. Wang, P. Ramuhalli, S. Cetiner, H. G. Kang, and M. Golay. (2021). "Prognostics and Health Management in Nuclear Power Plants: An Updated Method-Centric Review with Special Focus on Data-Driven Methods." *Frontiers in Energy Research*, 9, 696785. https://doi.org/10.3389/fenrg.2021.696785.

Youngblood, R. W. (2001). "Risk Significance and Safety Significance." *Reliability Engineering & System Safety*, 73(2), pp. 121–136. https://doi.org/10.1016/S0951-8320(01)00056-4.

Zhang, L., J. Lin, B. Liu, Z. Zhang, X. Yan, and M. Wei. (2019). "A Review on Deep Learning Applications in Prognostics and Health Management." in *IEEE Access*, vol. 7, pp. 162415-162438. https://doi.org/10.1109/ACCESS.2019.2950985.